Loosely Coupled GNSS and IMU Integration for Accurate i-Boat Horizontal Navigation

Cahyadi, M. N.,[1, 2, 3*] Asfihani, T.,[3] Mardiyanto, R.[4] and Erfianti, R.[1]

[1]Department of Geomatics Engineering, Institut Teknologi Sepuluh Nopember; Surabaya 60111, Indonesia, E-mail: cahyadi@geodesy.its.ac.id

[2]Research Center of Marine and Earth Science Technology, Directorate of Research and Community Service, Institut Teknologi Sepuluh Nopember; Surabaya 60111, Indonesia

[3]Department of Mathematics, Institut Teknologi Sepuluh Nopember; Surabaya 60111 , Indonesia

[4]Department of Electrical Engineering, Institut Teknologi Sepuluh Nopember; Surabaya 60111 , Indonesia

**Corresponding Author*

DOI: https://doi.org/10.52939/ijg.v18i3.2233

Abstract

Global Navigation Satellite System (GNSS) has been widely utilized as a navigation solution for a mobile vehicle, yet stand-alone GNSS is unable to achieve sufficient accuracy in some applications. For example, in aquatic environment, the accuracy position of Unmanned Surface Vehicle (USV) is affected by the wind, current, and waves dynamics. In this case, the integration of GNSS and Inertial Measurement Unit (IMU) is an approach that can be used to support USV localization to achieve an accurate navigation solution. This study integrates GNSS and IMU using Extended Kalman Filter (EKF) to process loosely coupled integration. The integration results show that the estimated x-position is 0.3058 m accurately and the y-position has an accuracy of 0.2780 m. Then, the loosely coupled integration results of EKF were compared with Unscented Kalman Filter (UKF) simulation in the previous studies. The integration of GNSS and IMU using EKF produces a higher RMSE value of 2D position and attitude angle than UKF Scenario I. However, due to the smoothing process, EKF can provide a visually smoother trajectory than UKF, although it has a significant difference from the observed trajectory. On the other hand, the linear velocity estimated by EKF shows better stability compared to UKF in both Scenario I and II.

1. Introduction

Generally, the Unmanned Surface Vehicle (USV) is designed as an unmanned ship, supported by several modules including the propulsion module, main controller, localization module, measurement system, collision avoidance module, and communication module (Peng et al., 2017). Researchers are becoming more interested in USVs as new kind of automated and unattended platform, especially as the amount of scientific application, military, and commercial domains like oil and gas exploration grows (Gao et al., 2019). One of the most critical characteristics in successfully completing a dangerous or time-consuming task with a USV is accurate navigation (or localization). Global Navigation Satellite System (GNSS) is the most commonly used navigation sensor in USV localization systems. In general, the built-in features of high-precision differential GNSS shows a better result compared to independent GNSS. However, it needs a base station that located nearby, which restricts the range of navigation and increases the expense of base station development as well (Abd Rabbou et al., 2014). Under open-air situations, the integrated navigation system which merges both Inertial Measurement Unit (IMU) and GNSS has been broadly applied in automobile navigation. This is caused by both natural and purposeful influence which affect GNSS signals, such as ionospheric anomalies, jamming and spoofing. On the other hand, the IMU is able to provide attitude output as well as position and linear velocity at a relatively high level with proper processing. However, one of IMU's main drawbacks is that errors accumulate quickly as time goes by.When GNSS is merged with IMU sensors, GNSS will show its ability to provide precise position and linear velocity data, but IMU has the ability to produce reliable attitude data.

Thus, the integrated navigation system will be able to overcome each other's shortcomings while maintaining high-accuracy information. GNSS is mainly used to compensate accumulated linear velocity and position errors due to IMU, and IMU shows a better method during the unavailability of GNSS signals. The fusion research for localization has been done previously by Deng et al., (2015) using Wi-Fi and Smartphone Inertial Sensors at indoor locations using the Extended Kalman Filter (EKF) method. The results obtained using the EKF method show that the average localization error can be minimized up to 74.9% compared to stand-alone localization. GNSS and Inertial Navigation System (INS) loosely coupled integration using EKF are also known to be able to reduce the three-dimensional Root Mean Square Error (3D RMSE: latitude, longitude, and altitude) by 5 m (Falco et al., 2012). The advantages of using EKF in GNSS and IMU fusion include relatively lower computational load compared to other nonlinear filtering methods (Kaviani et al., 2018), more stable tuning of the noise covariance concerning tuning parameters (Rhudy et al., 2011), and it works well in general situations (Wang et al., 2018).

This study presents a loosely coupled integration of GNSS and IMU to compensate for errors of both systems using the EKF for the USV localization system. The EKF approach is the most widely used and advanced method for estimating the system of integrated navigation, and it works effectively in most cases (situations). Because of its ease of implementation and low computational burden, the EKF is broadly used to predict navigation status. EKF works upon system linearization and measurement model using Taylor series expansion involving derivatives of Jacobian matrices. With such a method, the difficulty of nonlinear filtering might be solved effectively and a quasi-optimal estimate with acceptable accuracy can be obtained. Previous studies have compared the Unscented Kalman Filter (UKF) and EKF methods in land vehicle localization, but still, no one has compared the two for USV localization, especially at 6 Degrees Of Freedom (DOF). In this study, the results of loosely coupled integration using EKF then compared with the results of the UKF simulation based on the research by Cahyadi et al., (2021) (in draft) which uses 9 measurements data. The main contributions of this paper lies in the following aspects: (1) The processing the data generated from the recording by the water surface vehicle using the EKF and smoothing algorithm, (2) The results of the integration of GNSS and IMU using EKF are compared with the fusion results using the UKF script, (3) The accuracy of the fusion results is analyzed based on the variables of position, linear velocity, and attitude. EKF and smoothing algorithm was chosen because in the research by Cahyadi and Rwabudandi (2019) it was proven to be able to produce more accurate and smoother position than the use of stand-alone GNSS due to the smoothing algorithm.

2. Sensor Measurement

This section briefly introduces the GNSS and IMU sensors used in i-Boat localization system, the Loosely coupled integration scheme, and the EKF algorithm used to integrate GNSS and IMU data.

2.1 GNSS and IMU Data Acquisition

The i-Boat is a USV developed by Institut Teknologi Sepuluh Nopember (ITS) Surabaya to carry out several roles, such as shipping saving, logistics fulfillment, as well as defense and security functions. The i-Boat localization system is supported by GNSS and IMU sensors which are located on the top of USV i-Boat stand frame as shown in Figure 1(a). The Here3 GNSS installed on the i-Boat is capable to provide 3D fix mode positioning accuracy of 2.5 m. The GNSS utilizes the u-blox M8 high precision GNSS modules (M8P) receiver with a data update frequency of 8 Hz. Meanwhile, the IMU sensors used in i-Boat localization consist of accelerometer and gyroscope sensors. The accelerometer has an output data rate specification of 4-4000 Hz, while the output data rate for the gyroscope is 4-8000 Hz. Data acquisition was carried out during i-Boat initial launching on September 20, 2020, in the waters of Shipyard company in Madura, Indonesia. The location of data collection is shown in Figure 1(b) which is geographically located at 7.171562° South Latitude and 112.7174701° East Longitude. The environmental conditions and the movement of the USV i-Boat during its launching are clearly recorded in a video that can be accessed at the following link https://youtu.be/uPy6DD1_mDY. Before i-Boat was operated, the sensor calibrations were not carried out on either GNSS or IMU. Therefore, the sensor functions cannot be ascertained according to the manufacturer's specifications. Besides, the data unavailability regarding user selectable parameters during data collection has caused deficiencies in identifying the parameters that will be used for loosely coupled integration. Thus, this study used the IMU sensor parameters following the research by Shin (2005) as shown in Table 1.

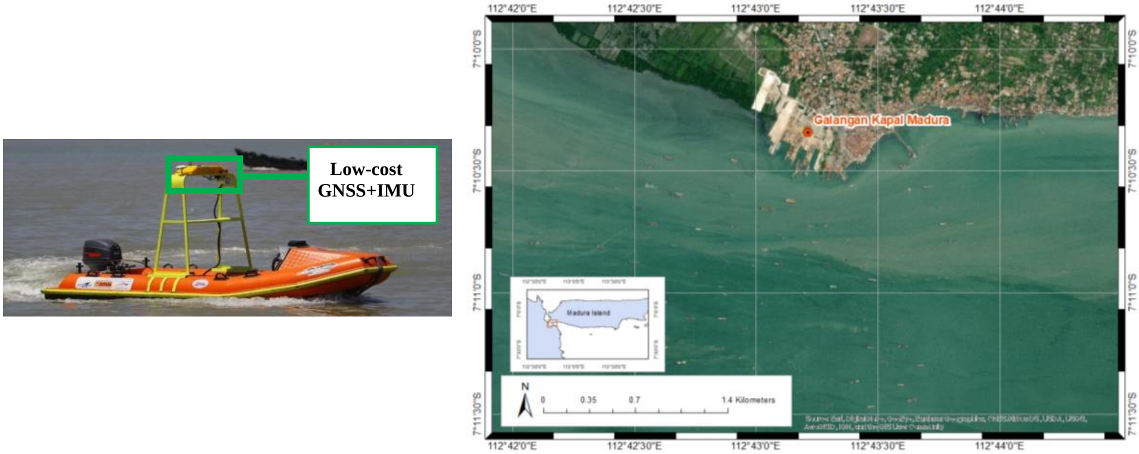

(a) (b)

Figure 1: (a) USV i-Boat using Low-cost GNSS and IMU as Localization System, (b) The location of data collection

Table 1: IMU Tuning Parameter

Parameter	Value
Gyroscope Bias	$0.5\frac{deg}{s}$, T = 1 hour
Accelerometer Bias	$0.05\frac{m}{s^2}$, T = 1 hour
Gyroscope Scale Factor	1000 PPM, T = 4 hours
Accelerometer Scale Factor	1000 PPM, T = 4 hours
Velocity random walk (VRW)	$0.6\frac{\frac{m}{s}}{\sqrt{hour}}$
Angular random walk (ARW)	$3.5\frac{deg}{\sqrt{hour}}$

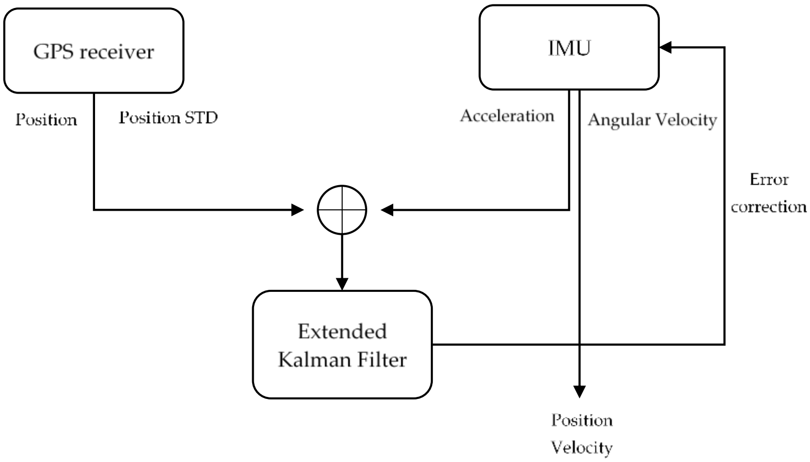

Figure 2: Scheme of the GNSS/IMU loosely coupled integration using EKF

2.2 Loosely Coupled Integration

Based on the scheme of loosely coupled integration, there is no effort to correct the GNSS signals from its errors. The loosely coupled sensor integration system covered in this paper is described in Figure 2. The integral Kalman filter creates a state vector estimation based on the GNSS receiver data, which is then used to correct the IMU data; simultaneously, a connecting block appeared between them where the so-called integral Kalman filter generates the state vector prediction based on the GNSS receiver data. This prediction is used to correct the data from IMU. Table 2 shows the structure of input and output data in loosely coupled integration using EKF which has been conducted in this research.

Table 2: Input and Output Data of Loosely Coupled Integration EKF

Input			Output		
GNSS Data	IMU Data				
Time (s)	Time (s)	Acc x (m/s^2)	Time (s)	Roll (deg)	Vx (m/s)
Lat (deg)	Gyro x (rad/s)	Acc y (m/s^2)	Lat (deg)	Pitch (deg)	Vy (m/s)
Lon (deg)	Gyro y (rad/s)	Acc z (m/s^2)	Lon (deg)	Yaw (deg)	Vz (m/s)
z (m)	Gyro z (rad/s)		z (m)		

2.3 Filtering Algorithm

EKF is a recursive filter to estimate the state of a dynamic system from several noisy measurements, which were developed from the Standard Kalman Filter to overcome nonlinear dynamic systems. At each time step, the primary principle of EKF is to linearize the nonlinear functions of the state equation and measurement function.This study used EKF algorithm in conducting loosely coupled GNSS and IMU integration to minimize the variance estimation. The EKF algorithm is summarized as the following steps:

Step Time update:

$$x_{k+1|k} = A_{k+1}x_{k|k}$$

Equation 1

$$P_{k+1|k} = A_{k+1}P_{k|k}{A_{k+1}}^T + Q_{k+1}$$

Equation 2

Step Calculate Kalman Gain:

$$K_{k+1} = P_{k+1|k}{H_{k+1}}^T(H_{k+1}P_{k+1|k}{H_{k+1}}^T + R_{k+1})^{-1}$$

Equation 3

Step Measurement Update:

$$x_{k+1|k+1} = x_{k+1|k} + K_{k+1}(z - H_{k+1}x_{k+1|k})$$

Equation 4

$$P_{k+1|k+1} = P_{k+1|k} - K_{k+1}H_{k+1}P_{k+1|k}$$

Equation 5

Where x is the state matrix, A_{k+1} is the state transition matrix, which is the Jacobian matrix of the nonlinear function **f(.)**, P is the error covariance, Q is the noise process covariance, H_{k+1} is the measurement matrix, which is the Jacobian matrix of the nonlinear function **h(.)**, K_{k+1} is the Kalman gain, R is the measurement covariance, and z is the measurement matrix. Both models of the system process and the measurement should be arranged in linear throughout the creation of the EKF. The "first order" approximations to the optimal terms are provided by the linearization technique. These approximations in the mean and covariance of the state estimation produce second order errors, and filter divergence might occur as a result (Cahyadi and Rwabudandi, 2019). Then, the EKF equations are used after the linear model has been generated. The time update stage projects the current state and error covariance forward to obtain a priori estimates for the next stage. The main purpose of EKF is to minimize the covariance error at the measurement update stage, therefore Kalman Gain needs to be calculated first. The last stage of the EKF incorporates new measurements into the a priori estimate to get a more accurate a posteriori estimate.

3. Application of the EKF in GNSS/IMU Loosely Coupled Navigation System

The following section describes the state vector and the function of nonlinear state transition for EKF regarding the loosely coupled integration of GNSS/IMU and its simulation result.

3.1 State Vector and State Transition Function

The error state vector of a GNSS/IMU tightly coupled integration using EKF is stated below:

$$\delta x = \left[(\delta r^c)^T \ (\delta v^c)^T \ \psi^T \ b_g^T \ b_a^T \ s_g^T \ s_a^T \ \gamma_g^T \ \gamma_a^T \ \right]$$

Equation 6

Where δr^c and δv^c can be written as follows:

$$\delta r^c = [\delta r_N \ \delta r_E \ \delta r_D]^T$$

Equation 7

$$\delta v^c = [\delta v_N \ \delta v_E \ \delta v_D]^T$$

Equation 8

ψ denotes the attitude errors; b_g the gyro biases; b_a the accelerometer biases; s_g represents the gyro scale factors; s_a denotes the accelerometer scale factors; and γ_g and γ_a are non-orthogonalities of the gyro and accelerometer triad, respectively. Thus, the system noise vector is presented as:

$$w = \left[w_v^T \ w_\psi^T \ w_{gb}^T \ w_{ab}^T \ w_{gs}^T \ w_{as}^T \ w_{g\gamma}^T \ w_{a\gamma}^T\right]^T$$

Equation 9

where w_v and w_ψ are the velocity and the attitude noise; w_{gb} and w_{ab} represent the bias noise of the gyros and accelerometers; w_{gs} and w_{as} are noise of the gyro and accelerometer scale factor; $w_{g\gamma}$ and $w_{a\gamma}$ are noise of the gyro-triad and accelerometer-triad non-orthogonalities.

ISSN: 1686-6576 (Printed) | ISSN 2673-0014 (Online) | © Geoinformatics International

3.2 GNSS and IMU Integration

This section describes the simulation of GNSS and IMU loosely coupled integration based. Raw IMU data and GNSS data were retrieved during the initial launching of i-Boat. During the launch of the i-Boat, GNSS and IMU data were captured, and the navigation solutions were executed in post-processing on the laptop's recorded data. The results of the estimated solutions are evaluated relative to the observation data. The trajectory estimation resulted from loosely coupled integration are shown in Figure 4. Generally, the result of trajectory estimation was well aligned with observation data, with some parts that seem smoother than the observation data due to the smoothing algorithm. The algorithm works by merging forward and backward filter solutions to create an ideal estimate based on the whole past, current, and future observations. The computational smoothing procedure is shown in Figure 3. The time-series graph of the estimation results for the x and y positions is shown in Figure 5 seems to experience estimates that are getting further away from the observation data as time goes by. The EKF performance in providing positional accuracy cannot be carried out on Differential-GNSS (DGNSS) references or certain station references due to insufficient data. Therefore, the accuracy is calculated on the observation data based on Root Mean Square Error (RMSE) formula. The RMSE values and maximum residuals for positions x and y as a result of loosely coupled integration are shown in Table 3. The maximum residual is the largest differences between estimated variable and observed variable.

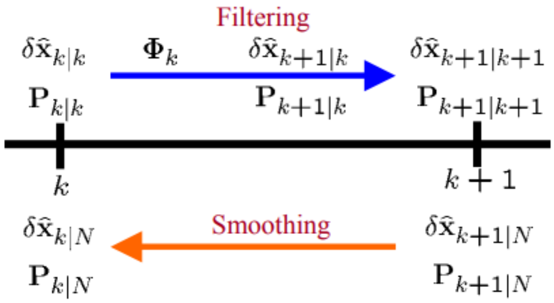

Figure 3: Smoothing computation Scheme (Shin, 2005)

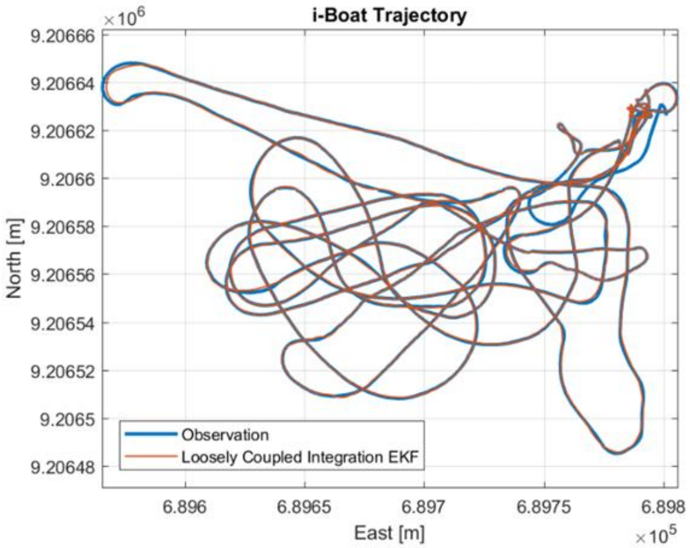

Figure 4: The trajectory result of loosely coupled integration EKF

Table 3: RMSE and Max. Residual of loosely coupled integration EKF

Positions	RMSE (m)	Max Residual (m)
x	0.3058	1.7559
y	0.2780	1.4551

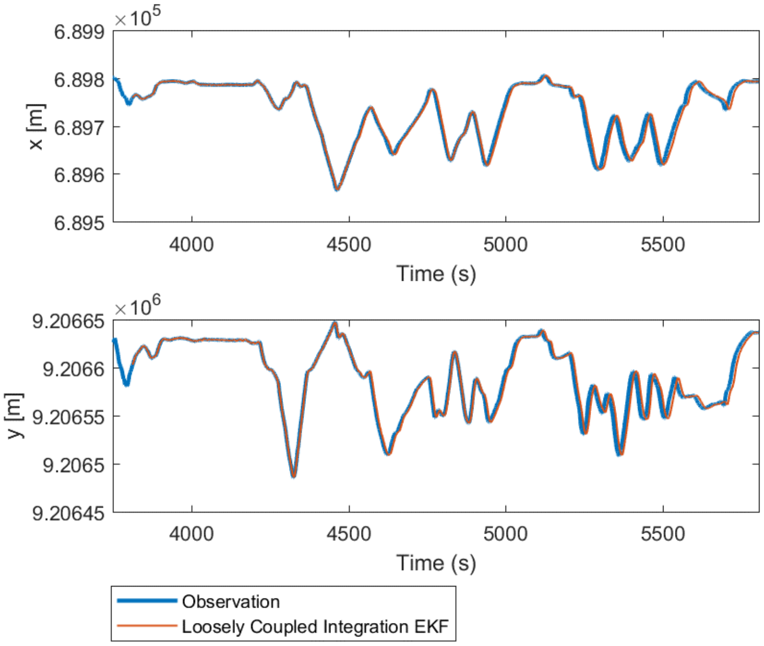

Figure 5: The time series of x and y position

4. Discussion

Loosely coupled integration has also been carried out in the research by Cahyadi et al., (2021) (in draft) using UKF algorithm. The integration of GNSS and IMU is based on USV movement at 6 DOF. The state vector and measurement model in UKF simulation were compiled based on the dynamic and kinematic model of USV movement in wide waters by differentiating the forces acting on the i-Boat (see Table 1.SM). The UKF simulation flow starts from the initialization stage, sigma point calculation, state prediction, measurement update, and Kalman Gain calculation until state estimation as shown in Figure 1. SM. The UKF simulation consists of 2 simulations, namely in Scenario I and Scenario II. Scenario I used 9 variables of observation data while Scenario II only used 6 variables of observation data by excluding attitude observation data. The comparison of 2D accuracy of integration results using EKF and UKF is presented in Table 4, which is the accuracy value calculated from the observation data. The 2D accuracy is calculated by:

$$\sigma_{2D} = \sqrt{\boldsymbol{RMSE_x}^2 + \boldsymbol{RMSE_y}^2}$$

Equation 10

In general, UKF simulation provide better results of 2D accuracy than EKF estimation, which only achieve accuracy of 0.4132 m. The accuracy of UKF Scenario II which uses less observational data than UKF Scenario I produces better accuracy because the attitude data contains a large amount of noise. Although the EKF accuracy is lower than the accuracy generated by UKF simulation, the EKF has shown a smoother trajectory visually than UKF because of the presence of smoothing process in EKF. There is a significant difference in one of the trajectory part of EKF and UKF estimation results as shown in Figure 6. Integration of GNSS and IMU using EKF is able to produce smoother and more stable trajectories than the observation data. The forward and backward filtering strategy was created to smoothen the EKF estimation output. Besides, it caused by the appearance of smoothing algorithm in EKF integration, EKF is known to be more stable against low covariance tuning noise (Rhudy et al., 2011). The EKF modification also shows good stability in overcoming large initial yaw angle errors (Jane, 2018) and produces state and internal parameter estimates (Wang et al., 2019). Smoothing is done by using data up to the current timestep to estimate the state of the USV. To make the initial value smoother, smoothing is done by using the localized EKF result directly. Then the smoothing trajectory uses span as the number of points used to calculate the current state estimate. In some cases, the existence of smoothing algorithms provides slightly better estimates but tends to be more sensitive about numerical accuracy, process, and noise measurements (Ko et al., 2018).

Table 4: Horizontal Accuracy Positioning

Accuracy	EKF	UKF Scenario I	UKF Scenario II
2D (m)	0.4132	0.1048	0.0402

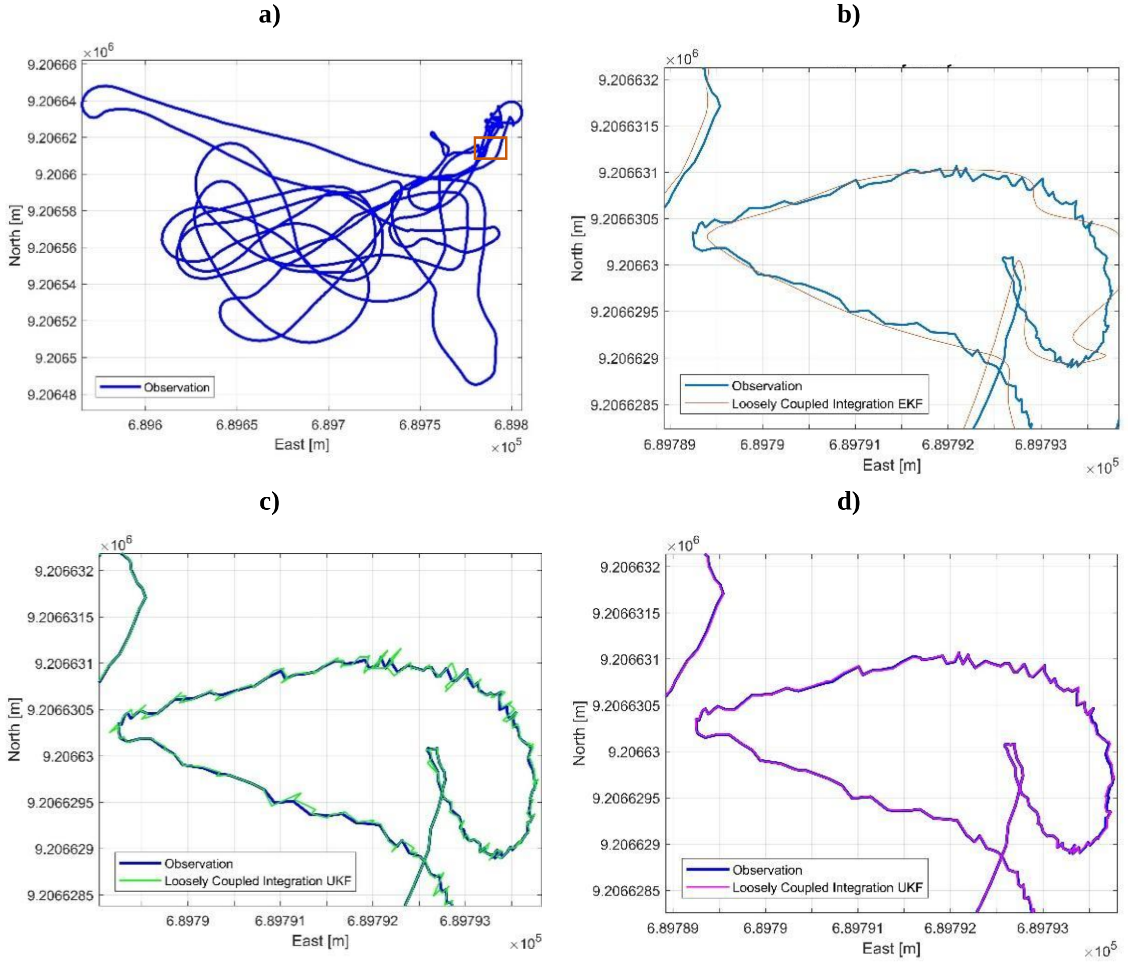

Figure 6: The significant trajectory difference of EKF and UKF: (a) the whole observation trajectory; (b) the magnified EKF estimation trajectory; (c) the magnified UKF Scenario I estimation trajectory; (d) the magnified Scenario II estimation trajectory

On the other hand, UKF Scenario II produces a rougher trajectory than the observation data, since there is no smoothing algorithm can be found in UKF.

The comparison of the attitude estimation results is shown in Figure 7 showing that UKF Scenario I has the best estimation performance, where the estimation results are closer to the attitude observation data. Meanwhile, UKF Scenario II shows a fluctuating trend over a long period of time compared to EKF. Compared to UKF estimation, EKF estimation results are more volatile, mainly in the pitch and yaw estimation. The stability attitude estimation in the UKF Scenario I can be achieved because there is attitude measurement data in the measurement model as part of the update stage of the UKF. The existence of data in the measurement model can provide accurate estimates of the variables that correspond to the data (Kaviani et al., 2018). The RMSE values and standard deviations are shown in Table 5 confirm that UKF Scenario I estimates the most accurate attitude compared to UKF Scenario II and EKF with the smallest RMSE values and standard deviations. Both UKF simulations by Cahyadi et. al., (2021) (in draft) and EKF processing in this study did not use linear velocity measurement data. However, both of them estimated the linear velocity as shown in Figure 8.

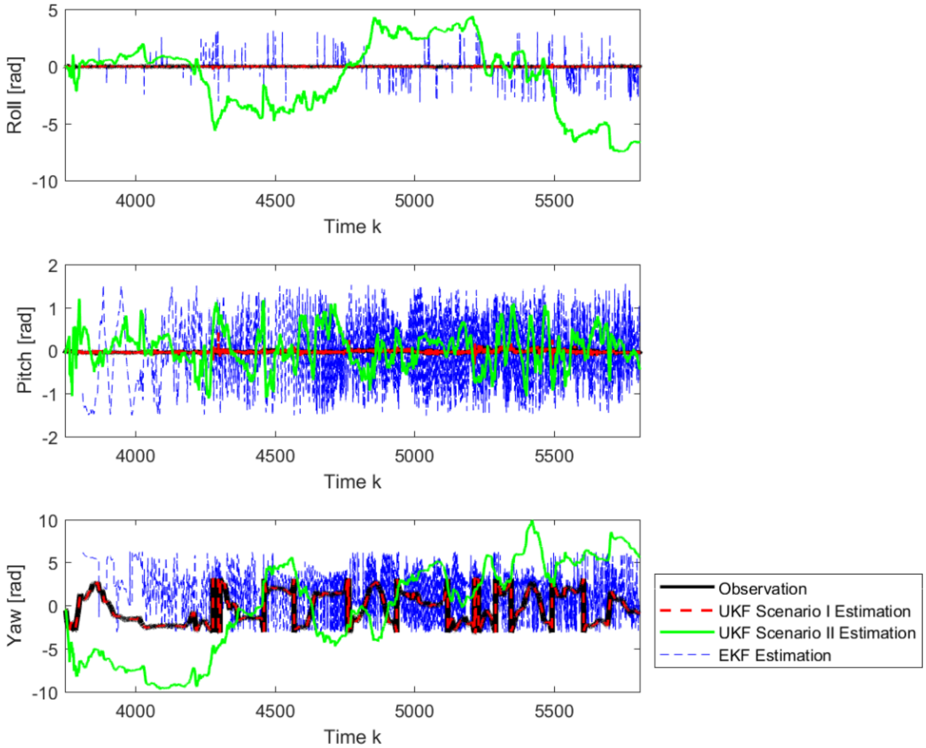

Figure 7: The significant difference attitude estimation of EKF and UKF

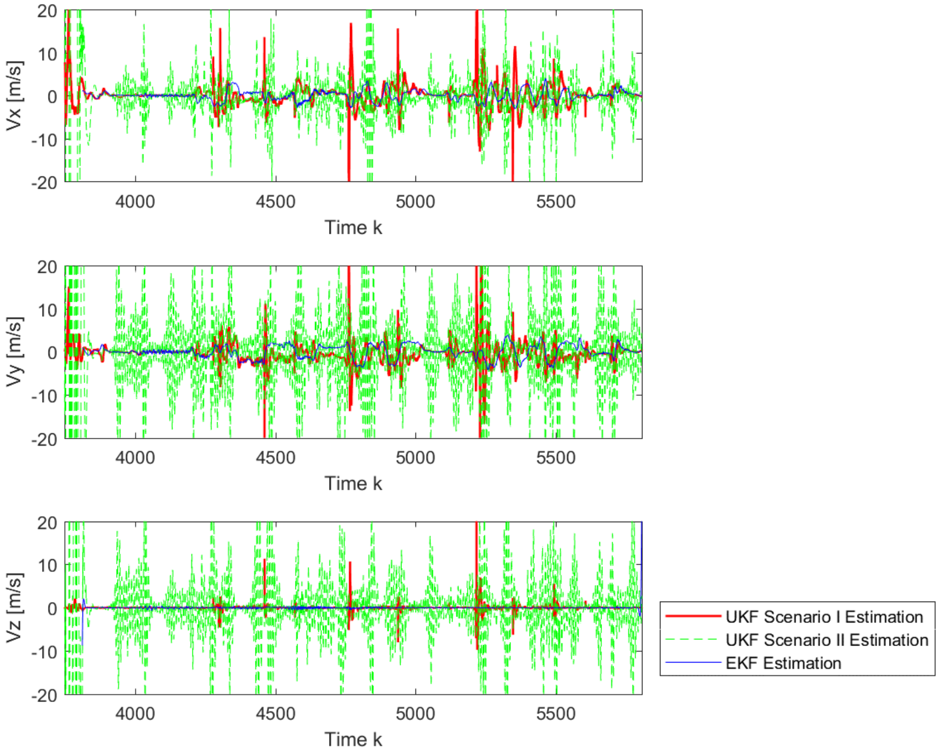

Figure 8: The linear velocity estimation difference of EKF and UKF

Table 5: RMSE and Standard Deviation of Attitude Estimations

Filtering Method	Variables	RMSE (rad)	Standard Deviation (rad)
UKF Scenario I	Roll	0.0158	0.0367
	Pitch	0.0158	0.0369
	Yaw	0.0158	1.7881
UKF Scenario II	Roll	3.3500	3.2022
	Pitch	0.4481	0.4380
	Yaw	5.2373	5.3928
EKF	Roll	0.4787	0.4787
	Pitch	0.7639	0.7628
	Yaw	3.6549	2.6376

Table 6: Standard Deviation of Linear Velocity Estimation

Variables	Standard Deviation (m/s)		
	UKF Scenario I	UKF Scenario II	EKF
Vx	2.6936	265.4383	1.1797
Vy	2.8375	278.1957	1.5216
Vz	0.7905	197.1744	0.6018

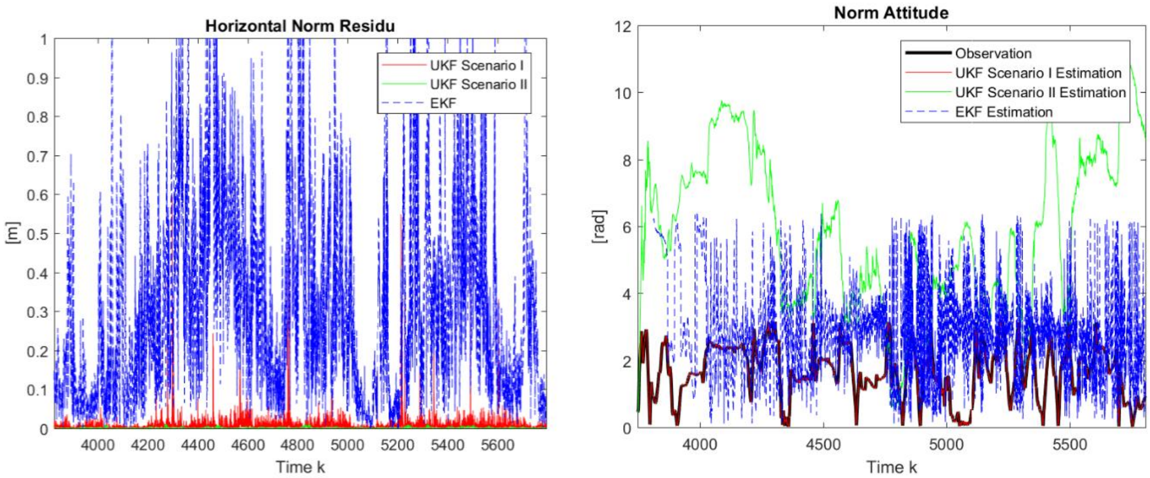

Figure 9: The significant difference of horizontal norm residual (right side) and norm attitude (left side)

The worst linear velocity estimation is shown by UKF Scenario II with a very volatile value. Meanwhile, EKF produces a more stable linear velocity estimation than UKF Scenario I, which sometimes produces peak estimates. Similar to the trajectory analysis in Figure 6, the linear velocity estimation in Figure 8 show that the EKF is more stable than the UKF when dealing with low covariance tuning noise (Rhudy et al., 2011). In Konatowsk and Pieni's (2007) study, the estimated linear velocity using EKF and UKF did not show a significant difference because the system noise was not too large. If there is a large noise jump in the system then it is possible that the filtering method used will give a poor linear velocity estimate. UKF Scenario II produces an linear velocity estimation with the largest standard deviation compared to UKF Scenario I and EKF both on the x, y, and z-axes as shown in Table 6.

For the comparison performance between EKF and UKF algorithms by Cahyadi et al. (in draft), the norm error estimation of the horizontal position (Δp) and attitude (ΔA) were chosen for this analysis and calculated using :

$$\Delta p = \sqrt{\Delta x^2 + \Delta y^2}$$

Equation 11

$$\Delta A = \sqrt{\Delta \phi^2 + \Delta \theta^2 + \Delta \psi^2}$$

Equation 12

The calculation result shows that EKF presents the most volatile estimation than both of UKF Scenario I and UKF Scenario II as shown in Figure 9.

Figure 9 (right side) shows that UKF produces estimation which tends to be stable with a narrower range of norm residual error than EKF estimation. A similar is shown in Figure 9 (left side), the norm attitude, from UKF is changed stable over time compared to EKF. Attitude estimation in UKF Scenario I simulation provides better accuracy than UKF Scenario II and EKF since the attitude measurement data was used in the simulation. Meanwhile, the attitude estimation on the EKF produced high- fluctuating estimation.

5. Conclusions

The EKF performance in this paper is assessed in a GNSS/IMU loosely coupled integration. The accurate prediction of EKF is examined towards observation data. The position accuracy of integration results show that the accuracy of the horizontal position of integration result is 0.413 m. The integration result using EKF were compared to the integration using UKF by Cahyadi et al., (2021) (in draft). The comparison of 2D accuracy shows that UKF produces more accurate estimation than EKF. However, the EKF estimation trajectory visually shows smooth results due to its smoothing algorithm. EKF produces estimation that is not as good as UKF in attitude estimation, because the value is very volatile. However, in linear velocity estimation, EKF produces a more stable estimation than the other 2 Scenario of UKF. EKF processing that has been carried out needs to be improved, especially in terms of attitude estimation. It is necessary to devise a solution that assesses the accuracy to the reference DGNSS or station reference in the future. Furthermore, it is necessary to investigate the case of GNSS outages to show the loosely coupled integration performance where the vehicle has to reach a high positioning accuracy while guaranteeing the safety of other vessels.

Funding

This study was funded by project scheme of Prototype Research DRPM ITS 2020 and Upgrade Tugas Akhir-Publication Writing-IPR Incentive Program (PPHKI) 2021.

Acknowledgments

The authors are grateful to the i-Boat ITS Team, the project scheme of Prototype Research DRPM ITS 2020 and Upgrade Tugas Akhir-Publication Writing-IPR Incentive Program (PPHKI) 2021 for the data and financial support of this study.

References

Abd Rabbou, M. and El-Rabbany, A., 2014, Tightly Coupled Integration of GPS-PPP and MEMS-Based Inertial System Using EKF and UKF. *GPS Solutions*, Vol. 19(4), DOI:10.1007/s10291-014-0415-3.

Cahyadi, M. N., and Rwabudandi, I., 2019, Integration of GNSS-IMU for Increasing the Observation Accuracy in Condensed Areas (Infrastructure and Forest Canopies). *E3S Web of Conferences*, Vol. 94, 1-4, DOI:10.1051/e3sconf/20199403015.

Cahyadi, M. N., Asfihani, T., Mardiyanto, R., Erfianti, R. and Jin, S., 2021, Performance of GPS and IMU Sensor Fusion Using Unscented Kalman Filter for Precise i-Boat Navigation in Infinite Wide Waters. (in draft).

Deng, Z. A., Hu, Y., Yu, J. and Na, Z., 2015, Extended Kalman Filter for Real Time Indoor Localization by Fusing WiFi and Smartphone Inertial Sensors. *Micromachines*, Vol. 6(4), 523-543.

Falco, G., Einicke, G. A., Malos, J. T. and Dovis, F., 2012, Performance Analysis of Constrained Loosely Coupled GPS/INS Integration Solutions. *Sensors*, Vol. 12(11), 15983-16007.

Gao, L., Gu, H. T. and Feng, L., 2019, Research on Submarine Buried Oil and Gas Pipeline Autonomous Inspection System of USV. *The 29th International Ocean and Polar Engineering Conference*. OnePetro. https://onepetro.org/IS-OPEIOPEC/proceedings-abstract/ISOPE19/All-ISOPE19/ISOPE-I-19-153/20970.

Hartikainen, J., Solin, A. and Särkkä, S., 2011, *Optimal Filtering with Kalman Filters and Smoothers.* Department of Biomedica Engineering and Computational Sciences. Aalto University School of Science.

Jane, H., 2018, *Comparison of EKF, EKF2 and UKF in a Loosely Coupled INS/GPS Integration*. Master's Thesis, Middle East Technical University. http://etd.lib.metu.edu.tr/upload/126-21808/index.pdf.

Kaviani, S., Salarieh, H., Alasty, A. and Abediny, M., 2018. Comparison of Nonlinear Filtering Techniques for Inertial Sensors Error Identification in INS/GPS Integration. *Scientia Iranica*, Vol. 25(3), 1281-1295.

Ko, N. Y., Youn, W., Choi, I. H., Song, G. and Kim, T. S., 2018, Features of Invariant Extended Kalman Filter Applied to Unmanned Aerial Vehicle Navigation. *Sensors*, Vol. 18(9), https://doi.org/10.3390/s18092855.

Konatowski, S. and Pieniężny, T., 2007, *A Comparison of Estimation Accuracy by the use of KF, EKF and UKF Filters*. Computational Methods and Experimental Measurements CMEM. 779-789. DOI:10.2495/CMEM070761.

Peng, Y., Yang, Y., Cui, J., Li, X., Pu, H., Gu, J., Xie, S. and Luo, J., 2017, Development of the USV 'JingHai-I'and Sea Trials in the Southern Yellow Sea. *Ocean Engineering*, Vol. 131, 186-196.

Rhudy, M., Gu, Y., Gross, J. and Napolitano, M., 2011, Sensitivity Analysis of EKF and UKF in GPS/INS Sensor Fusion. *AIAA Guidance, Navigation, and Control Conference*. DOI:10.2514/6.2011-6491.

Shin, E. H., 2005, *Estimation Techniques For Low-Cost Inertial Navigation*. UCGE Report, 20219.

Wang, M., Wu, W., He, X., Li, Y. and Pan, X., 2019, Consistent ST-EKF for Long Distance Land Vehicle Navigation Based on SINS/OD Integration. IEEE *Transactions on Vehicular Technology*, Vol. 68(11), 10525-10534.

Wang, M., Wu, W., Zhou, P. and He, X., 2018, State Transformation Extended Kalman Filter for GPS/SINS Tightly Coupled Integration. *GPS Solutions*, Vol. 22(4), 1-12.

Supplementary Material

Table 1.SM. Mathematical Modeling of Sensor Fusion using UKF (Cahyadi et. al. in draft)

Kinematic Model

$\dot{x} = u\ c\psi c\theta + v\ (-s\psi c\phi\ +\ c\psi s\theta s\phi\ ) + w\ \ (s\psi s\phi\ +\ c\psi c\phi s\theta\ )$ Equation 1

$\dot{y} = u\ s\psi c\theta + v\ (c\psi c\phi\ +\ s\phi s\theta s\psi) + w\ (-c\psi s\phi\ +\ s\theta s\psi c\phi)$ Equation 2

$\dot{z} = u\ (-s\theta) + v\ c\theta s\phi + w\ c\theta c\phi$ Equation 3

$\dot{\phi} = p + q\ t\theta s\phi + r\ t\theta c\phi$ Equation 4

$\dot{\theta} = q\ c\phi + r\ (-s\phi)$ Equation 5

$\dot{\psi} = q\ (\frac{s\phi}{c\theta}) + r\ (\frac{c\phi}{c\theta})$ Equation 6

In the equation:
s · = sin (·). c · = cos (·). dan t · = tan (·)
Dot notation state the derivation of time.

- x. y. z are the position of the surge. sway. and heave motions. respectively.
- ϕ. θ. ψ are the angle of roll. pitch. and yaw motions. respectively.
- u. v. w are the linear velocity in the surge. sway. and heave motions. respectively.
- p. q. r are the angular velocity in roll. pitch. and yaw motions. respectively.

Dynamic Model

$\dot{u} = \frac{X-(m+m_x)qw+(m+m_x)rv}{(m+m_x)}$ Equation 7

$\dot{v} = \frac{Y-(m+m_y)ru+(m+m_y)pw}{(m+m_y)}$ Equation 8

$\dot{w} = \frac{Z-(m+m_z)pv+(m+m_z)qu}{(m+m_z)}$ Equation 9

$\dot{p} = \frac{K-(I_{zz}-I_{yy})qr}{(I_{xx}+J_{xx})}$ Equation 10

$\dot{q} = \frac{M-(I_{xx}-I_{zz})pr}{(I_{yy}+J_{yy})}$ Equation 11

$\dot{r} = \frac{N-(I_{yy}-I_{xx})pq}{(I_{zz}+J_{zz})}$ Equation 12

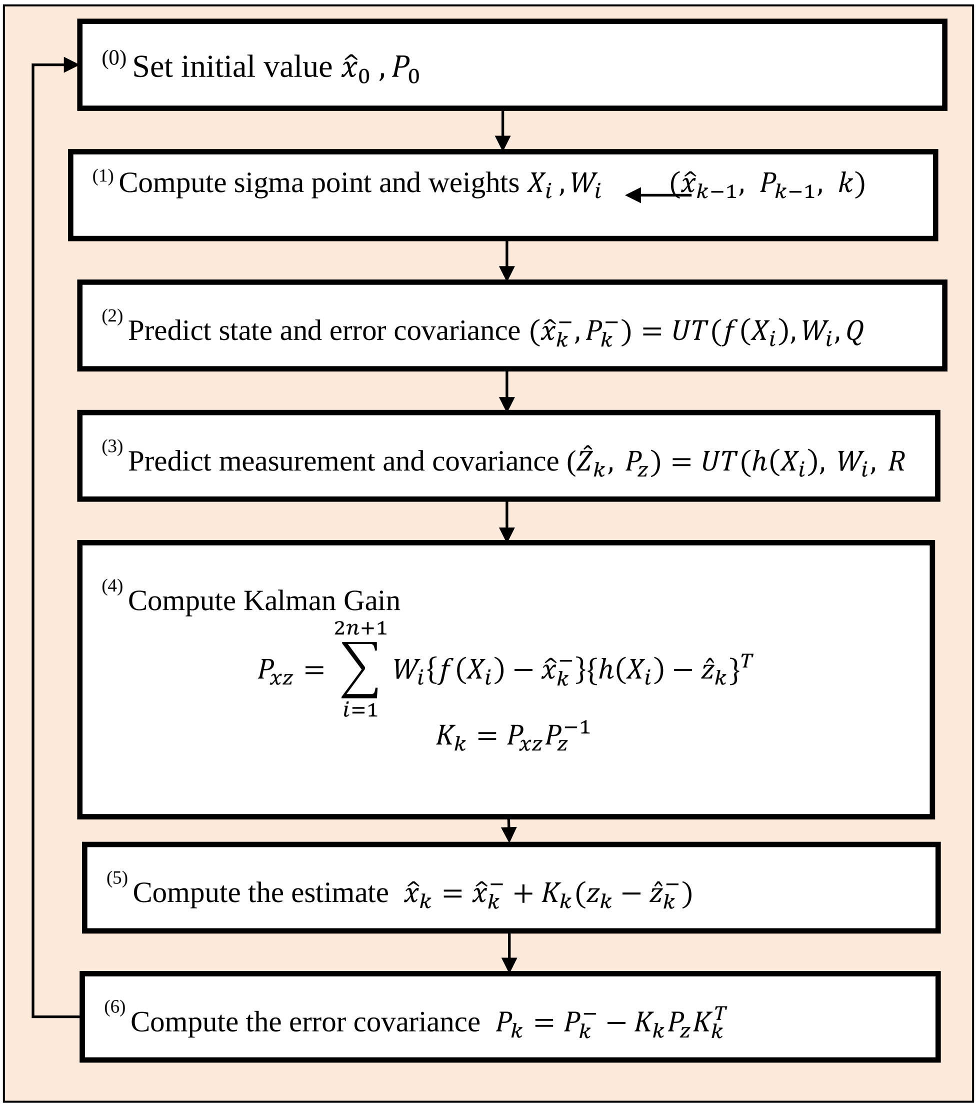

Figure 1SM: The UKF Algorithm

ISSN: 1686-6576 (Printed) | ISSN 2673-0014 (Online) | © Geoinformatics International